Modeling and Analysis of Source Contribution of PM_{10} during Severe Pollution Events in Southern Taiwan

W. C. Wang, K. S. Chen*

Institute of Environmental Engineering, National Sun Yat-Sen University, Kaohsiung 80424, Taiwan, ROC.

Abstract

This work simulates the hourly variations of PM_{10} (suspended particles with diameter < 10 μm) during severe pollution events in southern Taiwan (Kaohsiung City and Pingtung County) in spring, autumn and winter of 2005 by using the Air Pollution Model (TAPM). Comparisons between simulations and measurements at three sites (industrial, urban and rural) were satisfactory. The synoptic weather chart indicated that prevailing winds were northwest (spring), north (autumn), and northeasterly (winter). Meteorological conditions suggest that PM_{10} typically accumulated and triggered a pollution episode on days with high surface pressure and low winds. Estimations using the TAPM model suggest that point-source emissions were the predominant contributors (about 49.1%) to PM_{10} concentrations at Hsiung-Kong site industrial site in Kaohsiung City, followed by area sources (approximately 35.0%) and transport from neighboring areas (7.8%). Because Pingtung City (urban) and Chao-Chou town (rural) are located downwind of Kaohsiung City when north or northeasterly winds prevail, the two sites also experience severe pollution events despite the lack of industrial sources; transport from neighboring areas contributed roughly 39.1% to PM_{10} concentrations at Pingtung site and 48.7% at Chao-Chou site. Since traffic emissions contributed little (around 8%) to PM_{10} concentrations at the three sites, reducing PM_{10} emissions from industrial sources in Kaohsiung City should be an effective way of improving air quality for Kaohsiung City and downwind areas such as Pingtung County.

Keywords: TAPM; Particulate matter; PM_{10}; Air pollution modeling; Source contribution; Meteorological condition.

INTRODUCTION

Kaohsiung City, in southern Taiwan, is a heavily industrialized harbor city, with an area of 153.6 km^2 and a population of 1.49

* Corresponding author. Tel.: +886-7-5254406; Fax: +886-7-5254406

E-*mail address*: shin@mail.nsysu.edu.tw

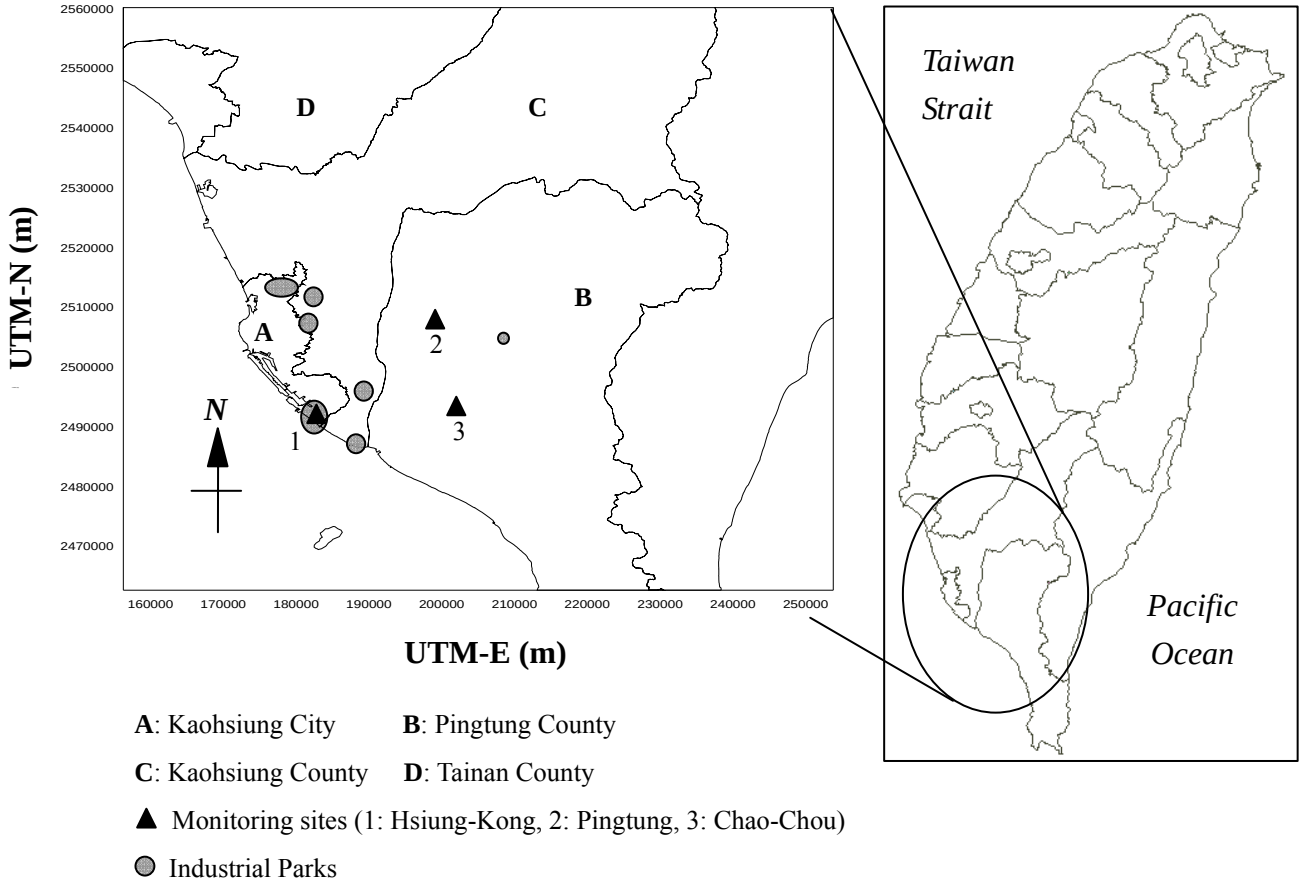

Fig. 1. Model domain and the three monitoring sites in southern Taiwan.

million. Six major industrial parks are located in and around Kaohsiung City (Fig. 1). These parks are home to oil refineries, petrol/plastic industries, power plants, iron/steel/metal plants, recycling factories, and large municipal waste incinerators. Due to intensive industrial and traffic activities, the Kaohsiung metropolitan area has the poorest air quality in Taiwan – either increased ground-level concentrations of particulate matter (PM) or ozone (O_3) associated with unfavorable meteorological conditions – particularly between late fall and mid-spring (Chen *et al.,* 2004). Pingtung County, to the south of Kaohsiung City, is primarily agricultural with several small industries located in northern Pingtung County. However, air quality in northern (e.g., Pingtung City) and central (e.g., Chao-Chou town) Pingtung County is as bad as that in the Kaohsiung area, despite the fact that population densities, traffic volumes and industrial emissions in Pingtung County are significantly lower than those of the Kaohsiung area. This poor air quality is mainly because northern and central Pingtung County are downwind of the Kaohsiung area when north or northeasterly winds prevail typically in autumn and winter (Chen *et al.*, 2003, 2004).

Primary PM is emitted directly into the

atmosphere by anthropogenic sources (e.g., industry, vehicles, combustion sources, bare lands and open burnings), and natural sources (e.g., volcanic eruptions, wildfires and marine aerosols). Atmospheric PM can carry acids and toxic species (e.g., polycyclic aromatic hydrocarbons and heavy metals) and can have adverse effects on human health (Cheng *et al.*, 1996). Epidemiological studies have demonstrated a strong relationship between elevated concentrations of PM_{10} and mortality and morbidity (Lin and Lee, 2004; Arditsoglou and Samara, 2005). Identification of air pollution sources is important in developing clean-air strategies (So and Wang, 2004; Wang and Shooter, 2004; Viana *et al.*, 2006). In non-attainment areas, air-pollution models are frequently employed to predict hourly pollution levels and thereby help establish cost-effective means of reducing atmospheric PM concentrations and controlling emission sources (Park *et al.*, 2004; Zawar-Reza *et al.*, 2005; Luhar *et al.*, 2006; Wilson and Zawar-Reza, 2006; Cheng *et al.*, 2007).

In this work, hourly PM_{10} variations were simulated using TAPM-3.0 (Hurley, 2005) for severe pollution events during the three worst seasons (spring, fall, and winter) in Kaohsiung City and Pingtung County. Each simulation covers three consecutive days or 72 h. Measured data from three monitoring sites were collected and compared with simulation results. Meteorological conditions and source contributions at each monitoring site were analyzed.

MODEL DOMAIN AND MONITORING SITES

The three monitoring sites were Hsiung-Kong (industrial), Pingtung (urban) and Chao-Chou (rural) sites; all are located in southern Taiwan (Fig. 1). Taiwan's Environmental Protection Administration (EPA) has set up an air-quality monitoring station at each site that collect hourly air quality and meteorological data, including that for PM_{10} concentration, temperature and wind. Hsiung-Kong, with a population of approximately 151,932 and an area of 39.9 km^2, is adjacent to the Linhei Industrial Park at the southern end of Kaohsiung City. This industrial park is home to iron/steel industries, petrol/chemical plants, power plants, secondary aluminum sinter ovens and a large municipal waste incinerator. Since Kaohsiung International Airport is located in the Hsiung-Kong district, traffic density is usually very high.

Pingtung, which has a population of roughly 216,222 and an area of 65.1 km^2, is the capital of Pingtung County. Pingtung is primarily an administrative and business city. Chao-Chou has a population of about 57,189 and covers 42.4 km^2. It is primarily an agricultural rural town located in Pingtung County. Traffic density is generally low. The distance between the Hsiung-Kong and Pingtung monitoring sites is about 19 km, that between Pingtung and Chao-Chou sites is about 16 km, and that between Hsiung-Kong and Chao-Chou sites is about 23 km.

TAPM MODEL

Governing equations and grid setup

The Air Pollution Model (TAPM) is a three-dimensional, prognostic, Eulerian, incompressible, non-hydrostatic, primitive equation model in terrain-following coordinates for simulating atmospheric motion and pollutant transport using nested grids. Hurley *et al.* (2003) and Hurley (2005) described in detail the governing equations for mass, momentum, and energy, which are briefly elucidated as follows.

$$\frac{du}{dt}=\frac{\partial u}{\partial t}+(u,v)\cdot\nabla=\frac{\partial}{\partial x}\left(K_H\frac{\partial u}{\partial x}\right)+\frac{\partial}{\partial y}\left(K_H\frac{\partial u}{\partial y}\right)-\frac{\partial\overline{w'u'}}{\partial\sigma}\frac{\partial\sigma}{\partial z}-\theta_v\left(\frac{\partial P}{\partial x}+\frac{\partial P}{\partial\sigma}\frac{\partial\sigma}{\partial x}\right)+fv-N_s(u-u_s) \quad (1)$$

$$\frac{dv}{dt}=\frac{\partial v}{\partial t}+(u,v)\cdot\nabla=\frac{\partial}{\partial x}\left(K_H\frac{\partial v}{\partial x}\right)+\frac{\partial}{\partial y}\left(K_H\frac{\partial v}{\partial y}\right)-\frac{\partial\overline{w'v'}}{\partial\sigma}\frac{\partial\sigma}{\partial z}-\theta_v\left(\frac{\partial P}{\partial y}+\frac{\partial P}{\partial\sigma}\frac{\partial\sigma}{\partial y}\right)-fu-N_s(v-v_s) \quad (2)$$

$$\frac{\partial\dot{\sigma}}{\partial\sigma}=-\left(\frac{\partial u}{\partial x}+\frac{\partial v}{\partial y}\right)+u\frac{\partial}{\partial\sigma}\left(\frac{\partial\sigma}{\partial x}\right)+v\frac{\partial}{\partial\sigma}\left(\frac{\partial\sigma}{\partial y}\right) \quad (3)$$

$$\sigma=z_T\left(\frac{z-z_S}{z_T-z_s}\right) \quad (4)$$

In the above, t is time; (u, v) are horizontal winds; u_s and v_s are large-scale synoptic winds; σ is sigma-pressure; $\dot{\sigma}$ is vertical wind; z_T is the height of the top of the model; z_s is terrain height; K_H is the horizontal diffusion coefficient; $\overline{w'\phi'}$ is the eddy term; f is the Coriolis parameter; θ_v is the potential virtual temperature. The turbulence terms in Eqs. (1) and (2) are derived by solving equations for the turbulent kinetic energy and the eddy dissipation rate. The governing equation for species concentration, χ, such as PM_{10} is

$$\frac{d\chi}{dt}=\frac{\partial}{\partial x}\left(K_\chi\frac{\partial\chi}{\partial x}\right)+\frac{\partial}{\partial y}\left(K_\chi\frac{\partial\chi}{\partial y}\right)_\chi-\left(\frac{\partial\sigma}{\partial z}\right)\frac{\partial}{\partial\sigma}\left(\overline{w'\chi'}\right)+R_x+S \quad (5)$$

where K_χ is the diffusion coefficient; $\overline{w'\chi'}$ is the eddy term; R_χ is the chemical reaction term; S_χ is the pollutant emission term. The diffusion coefficient utilized for pollutant concentration is K_χ = 2.5 K, where K is the diffusion coefficient for the turbulent kinetic energy. Furthermore, 13 species are involved in ten reactions. These species are NO, NO_2, O_3, SO_2, hydrogen peroxide (H_2O_2), R_{smog}, radical pool (RP), stable non-gaseous organic carbon (SNGOC), stable gaseous nitrogen (SGN) products, stable non-gaseous nitrogen (SNGN) products, stable nongaseous sulfur (SNGS)products, Airborne Particulate Matter (APM), and Fine Particulate Matter (FPM), which comprises secondary particulate concentrations of SNGOC, SNGN and SNGS (Hurley, 2002). In this work, pollutant emission rates were considered and input to the model via boundary conditions (discussed later).

The TAPM is run on a personal computer

for simulating mesoscale atmospheric motions using nested grids with meteorological, geographical and air pollution components. Each horizontal layer had 35 × 35 grids, nested from the outside to the inside with size of 20, 7.5, 2 and 0.5 km. The entire simulation domain covered over 700 km × 700 km (Fig. 1); the fine grids covered the southern Taiwan over the domain of 262.5 km × 262.5 km, and were centered at 120°22' E and 22°23' N. The vertical domain was 8000 m high and comprised 25 horizontal layers at altitudes of 10, 25, 50, 100,150, 200, 250, 300, 400, 500, 600, 750, 1000, 1250, 1500, 1750, 2000, 2500, 3000, 3500, 4000, 5000, 6000, 7000 and 8000 m.

Emission inventory and boundary conditions

An emission inventory was obtained using TEDS-6.03 (2006), which was issued by Taiwan's EPA. Table 1 presents all emission rates of PM_{10}, sulfur dioxides (SO_2), nitrogen oxides (= NO + NO_2) and non-methane hydrocarbons (NMHC) from point (industrial), area and line (traffic) sources in each region. The methods of obtaining emission rates from various sources, except the updated emission rates in TEDS-6.03, were similar to those used by TEDS-4.2 (Chen *et al.*, 2003). However, reactive hydrocarbons, R_{smog}, replace the NMHC rate in the TAPM (Johnson, 1984), in which R_{smog} is defined as the product of a reactive coefficient (or a multiplicative factor) and NMHC emissions. A multiplicative factor of 0.0067 was used for converting the emission rates of NMHC to those of R_{smog} (Johnson, 1984), and a multiplicative factor of 1.0 was applied to emission rates of all other primary pollutants, such as PM_{10}, NO_x, and SO_2.

TAPM classifies the surface vegetation (land-use) into 29 classes. Surface data in the model were acquired using geographical charts that were issued by the Ministry of the Interior, Taiwan, to determine area fractions of land-use in each grid.

The TAPM model is initialized at each grid point with values for wind velocities, temperatures and humidity ratios that were interpolated from synoptic analyses. The initial pollutant concentrations at inflow boundaries on the outermost grids are set to background values, while zero-gradient conditions are applied at outflow boundaries. Background conditions for pollutants were set to 25 $\mu g/m^3$ for PM_{10}, 0.7 ppbv for R_{smog} (Hurley, 2003), 1 ppbv for SO_2 and 3 ppbv for NO_2 (Chang and Cardelino, 2000). Notably, the initial values of eddy terms were set to zero because of a thermally stable condition at midnight. Four-dimensional data assimilation (FDDA) was adopted to compare simulated surface winds with ground observations and correct horizontal momentum equations using the Newtonian relaxation (or nudging) procedure (Stauffer and Seaman, 1994; Hurley, 2002).

Model performance was assessed relative to actual measurements using the correlation coefficient (R) and index of agreement

Table 1. Emission rates of pollutants in TEDS-6.03 in southern Taiwan (kton per year)

			PM_{10}	SO_2	NO_x	NMHC
Kaohsiung City	Area Sources	Paved Road	12.148	0.000	0.000	0.000
		Unpaved Road	0.000	0.000	0.000	0.000
		Others	8.061	4.579	11.169	47.198
	Line Sources	Gasoline Vehicles	1.002	0.061	4.512	17.761
		Diesel Vehicles	1.064	0.179	6.720	1.142
	Point Sources		7.989	46.953	61.347	39.038
Kaohsiung County	Area Sources	Paved Road	8.607	0.000	0.000	0.001
		Unpaved Road	1.713	0.000	0.000	0.020
		Others	6.639	0.735	2.502	55.413
	Line Sources	Gasoline Vehicles	0.761	0.046	3.973	11.907
		Diesel Vehicles	1.373	0.230	7.923	0.946
	Point Sources		5.872	29.894	35.741	32.088
Pingtung County	Area Sources	Paved Road	7.965	0.000	0.000	0.000
		Unpaved Road	1.367	0.000	0.000	0.016
		Others	9.561	0.787	6.380	27.255
	Line Sources	Gasoline Vehicles	0.483	0.034	2.790	7.536
		Diesel Vehicles	0.706	0.127	3.827	0.550
	Point Sources		0.868	0.641	0.713	2.912
Tainan Area*	Area Sources	Paved Road	9.928	0.000	0.000	0.008
		Unpaved Road	1.481	0.000	0.000	0.046
		Others	14.740	1.010	2.570	46.231
	Line Sources	Gasoline Vehicles	0.713	0.054	4.360	8.540
		Diesel Vehicles	1.580	0.267	8.469	1.019
	Point Sources		4.659	10.437	6.744	35.028

* Tainan area includes Tainan City and Tainan County.

(*IOA*) as follows (Willmott *et al.*, 1985).

$$IOA = 1 - \frac{\sum_{i=1}^{N}\left(\left|P_i - O_i\right|\right)^2}{\sum_{i=1}^{N}\left(\left|P_i - \overline{O}\right| + \left|O_i - \overline{O}\right|\right)^2} \qquad (6)$$

where P_i and O_i are predicted and measured values, respectively, with sample size N, and $\overline{O}$ is average of measured data.

RESULTS AND DISCUSSION

Spring episodes (March 8–10, 2005)

Figs. 2(a)–(c) present a synoptic surface weather chart for March 9 and hourly variations in pressure and wind speed for March 8–10, 2005. A high-pressure system and northwest winds prevailed in southern Taiwan (Fig. 2(a)). Pressure was highest at approximately 1023.4 hPa on March 8 and lowest at about 1010.8 hPa on March 10 (Fig. 2(b)). Winds were low (< 4 m/s) during March 8–10, and were weaker than 2 m/s at most times (Fig. 2(c)). Notably, temperature was 13–28°C and relative humidity was 42–86% during this period.

Fig. 3(a) presents simulated surface wind vectors at 12:00 on March 9, 2005; the solid lines on the right of the plot represent

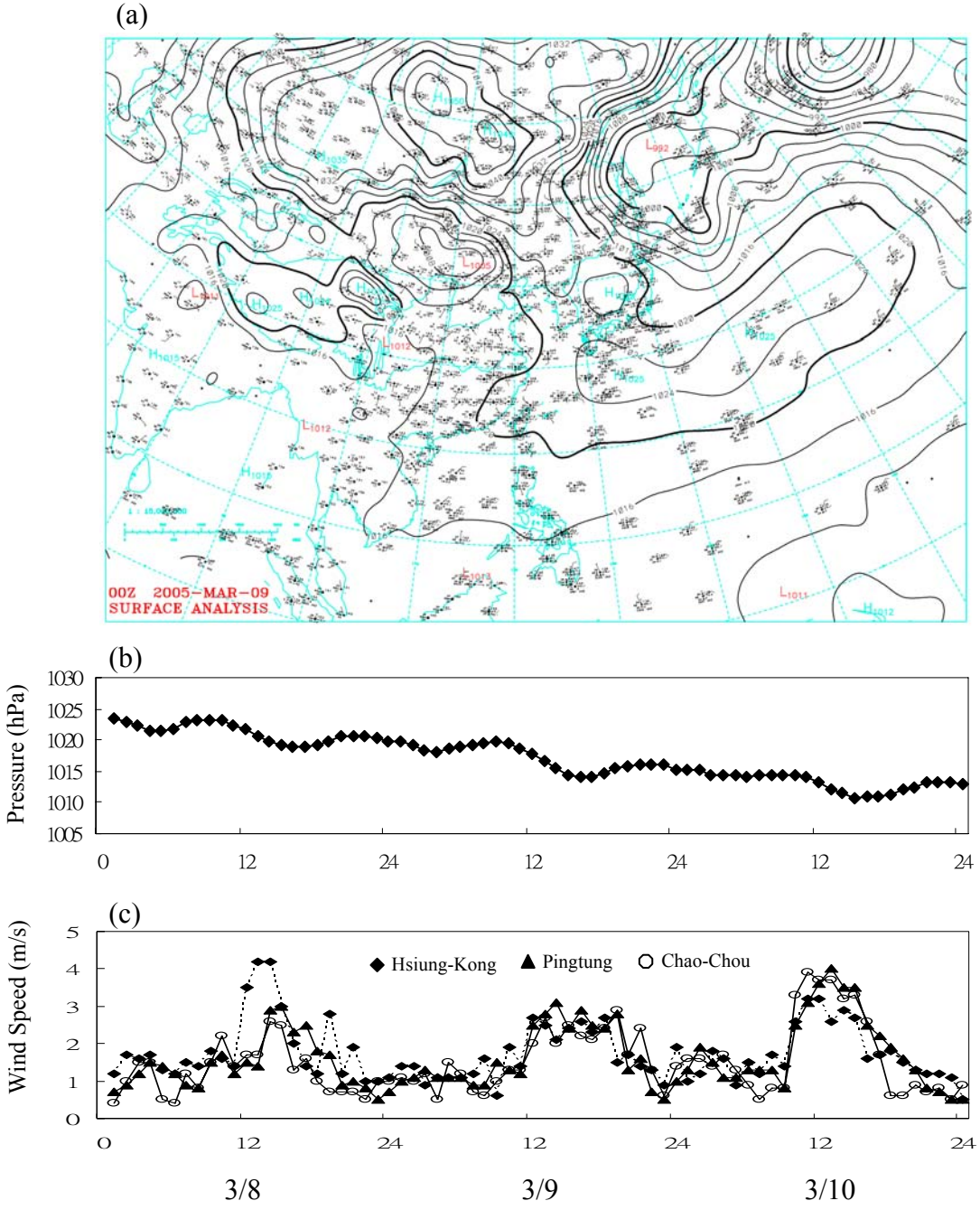

Fig. 2. (a) Synoptic surface weather chart on March 9, (b) hourly variations of pressure, and (c) hourly variations of wind speed on March 8–10, 2005.

mountain elevations – the highest elevation of approximately 2957 m. In Fig. 3(a), the relatively fast onshore winds from the northwest blew west inland at reduced speeds of 1.1–1.5 m/s. The corresponding concentration contours of PM_{10} reveal that a highly polluted location (> 120 μg/m^3) was near the costal lands (Fig. 3(b)); the three dark squares in Fig. 3(b) mark the monitoring sites of Hsiung-Kong, Pingtung

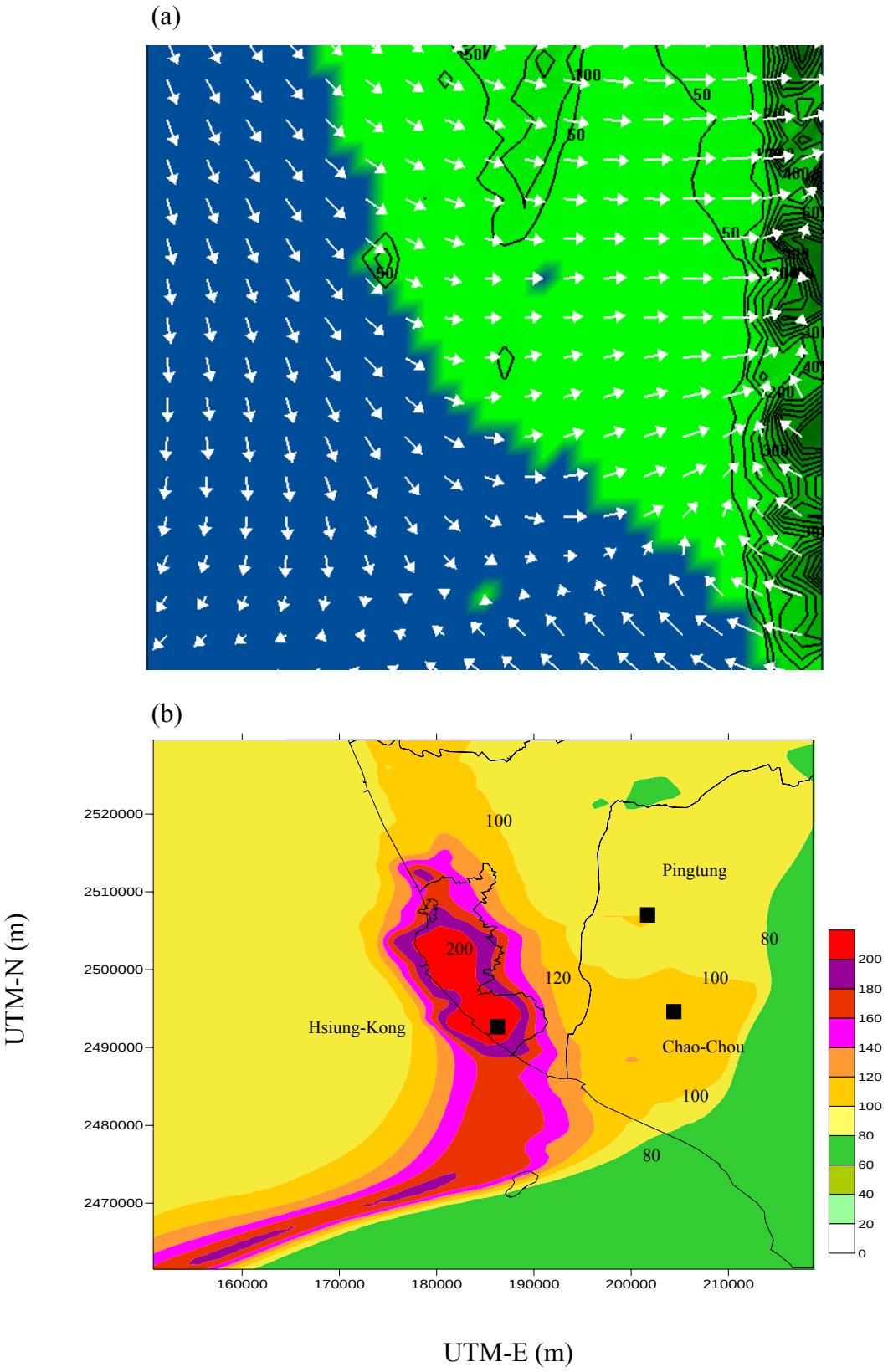

Fig. 3. (a) Simulated surface wind vectors, and (b) simulated concentration contours of PM_{10} at 12:00 on March 9, 2005.

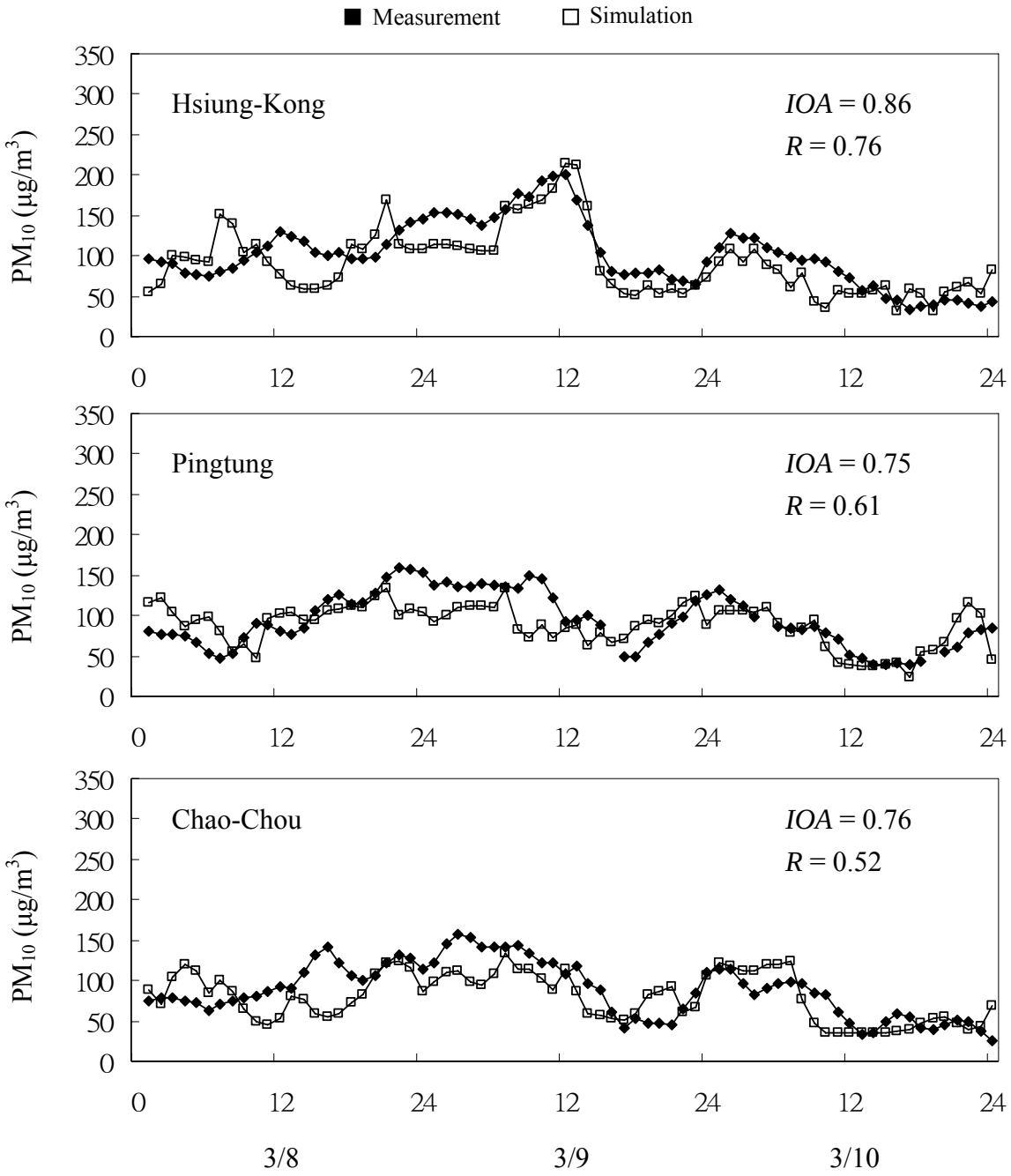

Fig. 4. Comparisons between hourly simulations of surface PM_{10} concentrations and measured concentrations at the Hsiung-Kong, Pingtung and Chao-Chou sites during March 8–10, 2005.

and Chao-Chou. More than 75% of Kaohsiung City was covered in $PM_{10} > 200$ μg/m^3. This highly polluted area extended downwind to the south; the PM_{10} concentration was 85 μg/m^3 at Pingtung site, northeast of the Hsiung-Kong site; and the PM_{10} concentration was 115 μg/m^3 at the Chao-Chou site, west of the Hsiung-Kong site. The PM_{10} concentrations were relatively low (< 80 μg/m^3) in the rural and

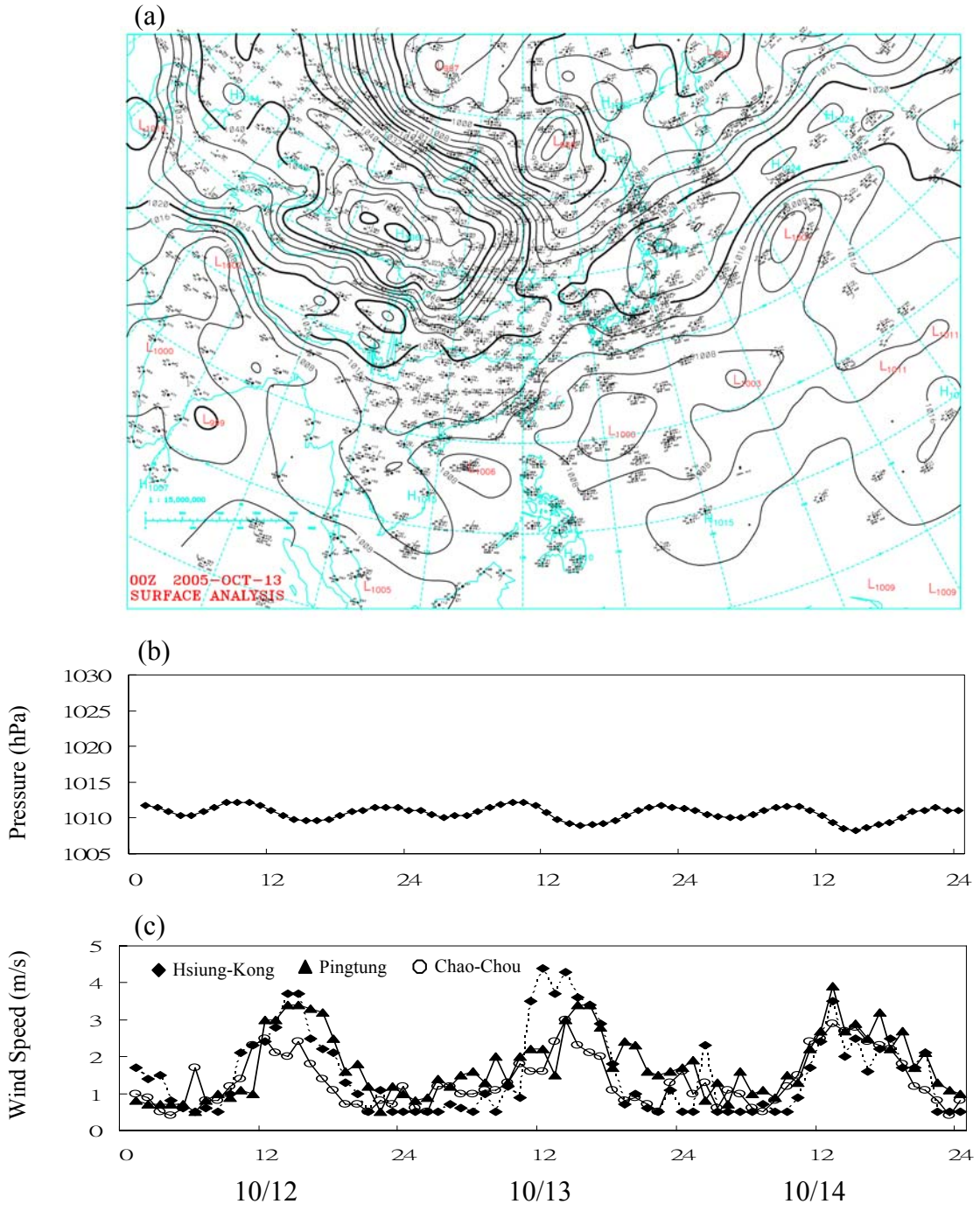

Fig. 5. (a) Synoptic surface weather chart on October 13, (b) hourly variations of pressure, and (c) hourly variations of wind speed on October 12–14, 2005.

mountainous regions.

Fig. 4 compares the 3-day hourly simulations of surface PM_{10} concentrations with measured values at Hsiung-Kong, Pingtung and Chao-Chou sites during March 8–10, 2005. These comparisons suggest that surface PM_{10} concentrations were usually high at midnight and in the early morning,

and were low in afternoon (around 16:00–18:00). The highest measured (and mean) concentration of PM_{10} was 215 (92) $\mu g/m^3$ at Hsiung-Kong, 135 (88) $\mu g/m^3$ at Pingtung, and 135 (80) $\mu g/m^3$ at Chao-Chou. These high PM_{10} events were strongly correlated with high-pressure systems and weak winds as a high surface pressure favors the descent of air parcels aloft and thus typically increases PM_{10} concentrations near the ground. Although predictions of model were in some cases higher or lower than measurements, simulated values were generally in agreement with measured values, with a correlation coefficient of R = 0.52–0.76, and an index of agreement (*IOA*) = 0.75–0.86. Notably, the agreement between predictions and measurements is regarded as good when *IOA* exceeds 0.5 (Hurley *et al.*, 2001 and 2003).

Autumn episodes (October 12–14, 2005)

Figs. 5(a) to 5(c) present a synoptic surface weather chart for October 13 and hourly variations in pressure and wind speed for October 12–14, 2005. A high-pressure system and north to northwest winds prevailed in southern Taiwan (Fig. 5(a)). Surface pressure was 1008.3–1012.1 hPa (Fig. 5(b)). Winds were frequently weak (< 2 m/s), particularly at midnight and in the early morning (Fig. 5(c)). Relatively strong winds of roughly 4 m/s were occasionally observed at 12:00–14:00. Notably, temperature was 26–32 ^oC and relative humidity was 57–88% during this period

Fig. 6(a) presents simulated surface wind vectors at 24:00 on October 24, 2005. The relatively fast onshore winds blew from the north to south-west or west to the inland at reduced speeds of 2.3–3.3 m/s, and then merged with downhill winds near the mountain base. The corresponding concentration contours of PM_{10} indicated that a highly polluted location (> 200 $\mu g/m^3$) near costal land extended from the southern part of Kaohsiung City to the west, resembling a banana in shape (Fig. 6(b)). The PM_{10} concentration was approximately 200 $\mu g/m^3$ at the Hsiung-Kong and Pingtung sites, and about 106 $\mu g/m^3$ at the Chao-Chou site at midnight.

Fig. 7 compares the 3-day hourly simulations of surface PM_{10} concentrations with measured values at the three sites during October 12–14, 2005. The PM_{10} concentrations were relatively high at midnight and in the early morning.

The highest (and mean) measured values were about 236 (123) $\mu g/m^3$ at Hsiung-Kong, 246 (105) $\mu g/m^3$ at Pingtung, and 129 (74) $\mu g/m^3$ at Chao-Chou. Similar to the case in spring, high PM_{10} events in autumn were related to high-pressure systems and weak winds. The simulated concentrations agreed reasonably well with measured values, with R = 0.47–0.56 and *IOA* = 0.69–0.75.

Winter episodes (December 16–18, 2005)

The synoptic surface weather chart for December 17 indicates that a high-pressure system with northeasterly winds prevailed over southern Taiwan (Fig. 8(a)). During December 16–18, 2005, surface pressure.

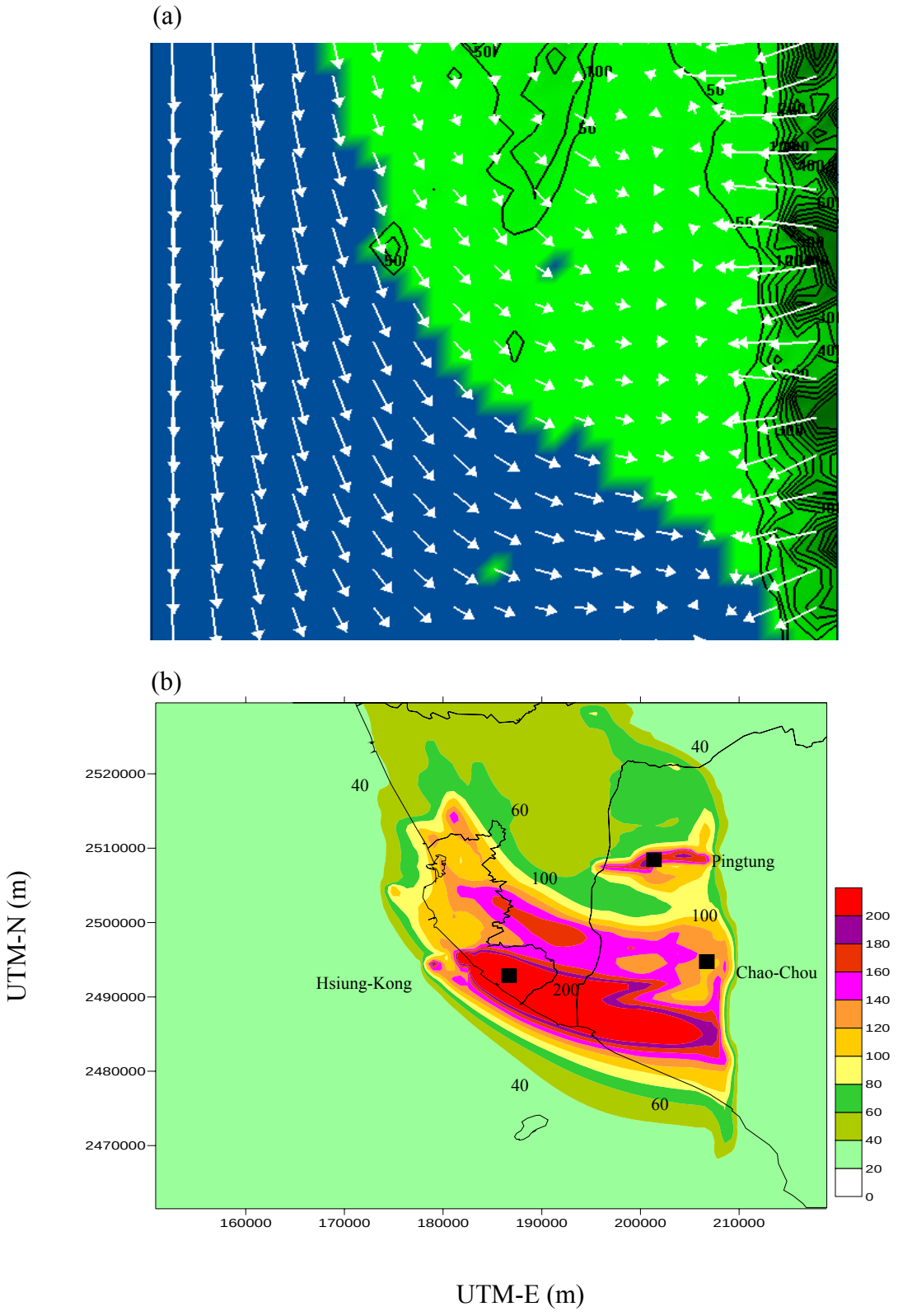

Fig. 6. (a) Simulated surface wind vectors, and (b) simulated concentration contours of PM_{10} at 24:00 on October 14, 2005.

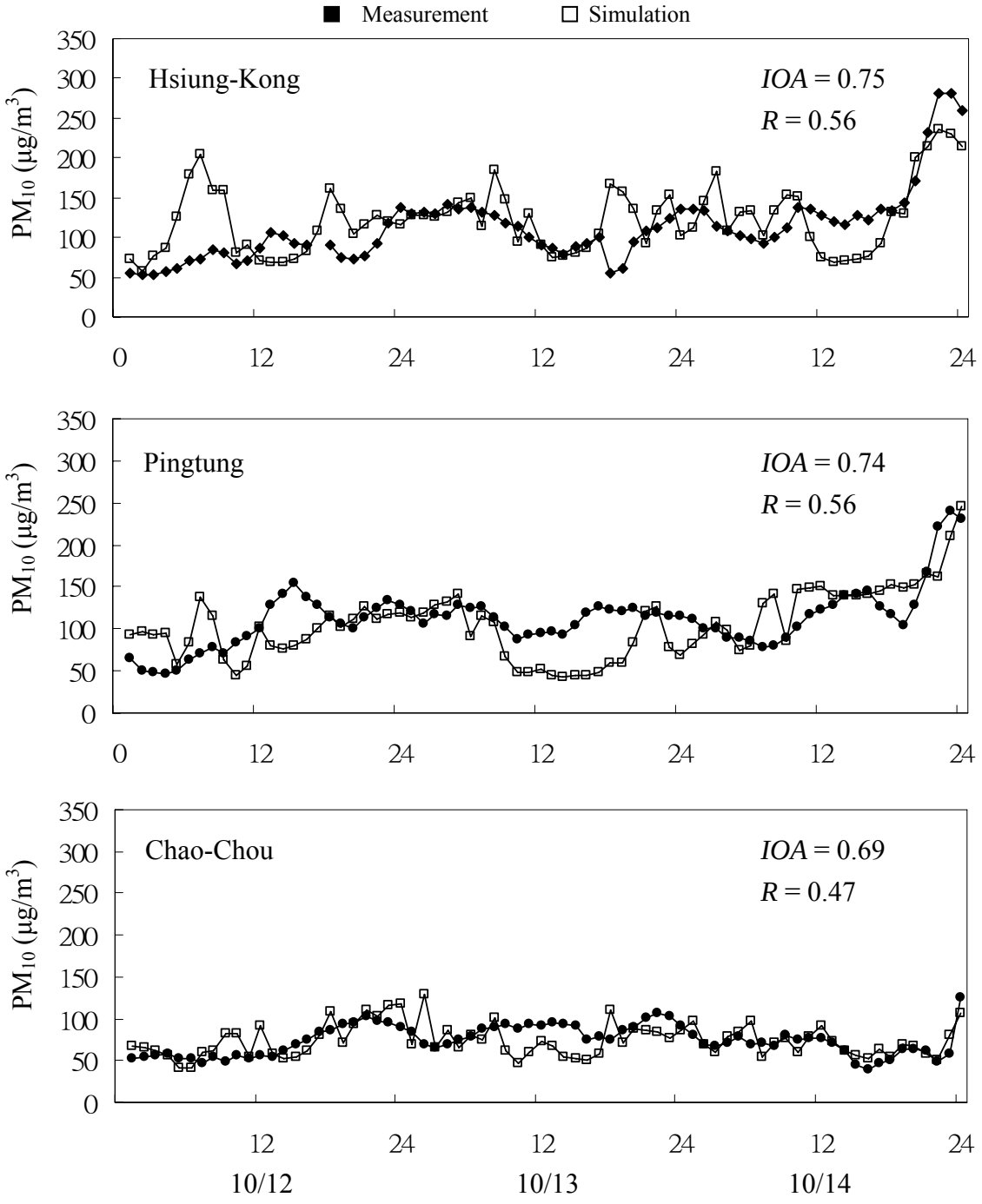

Fig. 7. Comparisons between hourly simulations of surface PM_{10} concentrations and measured concentrations at the Hsiung-Kong, Pingtung and Chao-Chou sites during October 12–14, 2005.

varied at 1019.0–1023.9 hPa (Fig. 8(b)), and winds were frequently weak (< 3 m/s) (Fig. 8(c)). Notably, temperature was 11–25°C and relative humidity was 44–80% during this period.

Simulated surface wind vectors at 20:00 on December 17, 2005 indicates that relatively strong north winds prevailed over

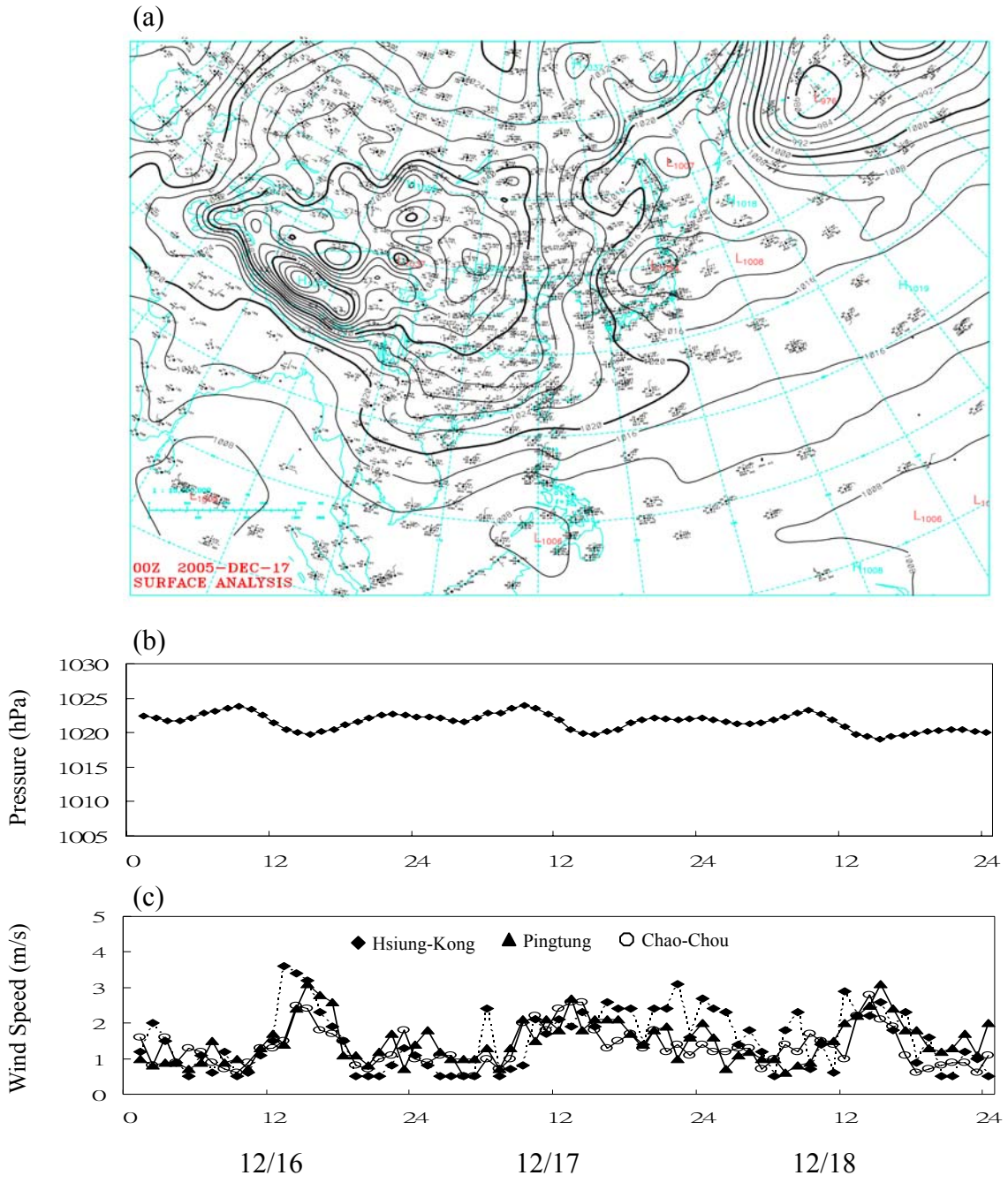

Fig. 8. (a) Synoptic surface weather chart on December 17, (b) hourly variations of pressure, and (c) hourly variations of wind speed on December 16–18, 2005.

the ocean (Fig. 9(a)), while relatively weak north to northwest winds prevailed inland and merged with downhill winds near the mountain base. Fig. 9(b) reveals that high-polluted regions (PM_{10} > 200 μg/m^3) located near coasts and mountain base, covering Kaohsiung City, Pingtung and Chao-Chou sites.

Fig. 10 compares the 3-day hourly simulations of surface PM_{10} concentrations

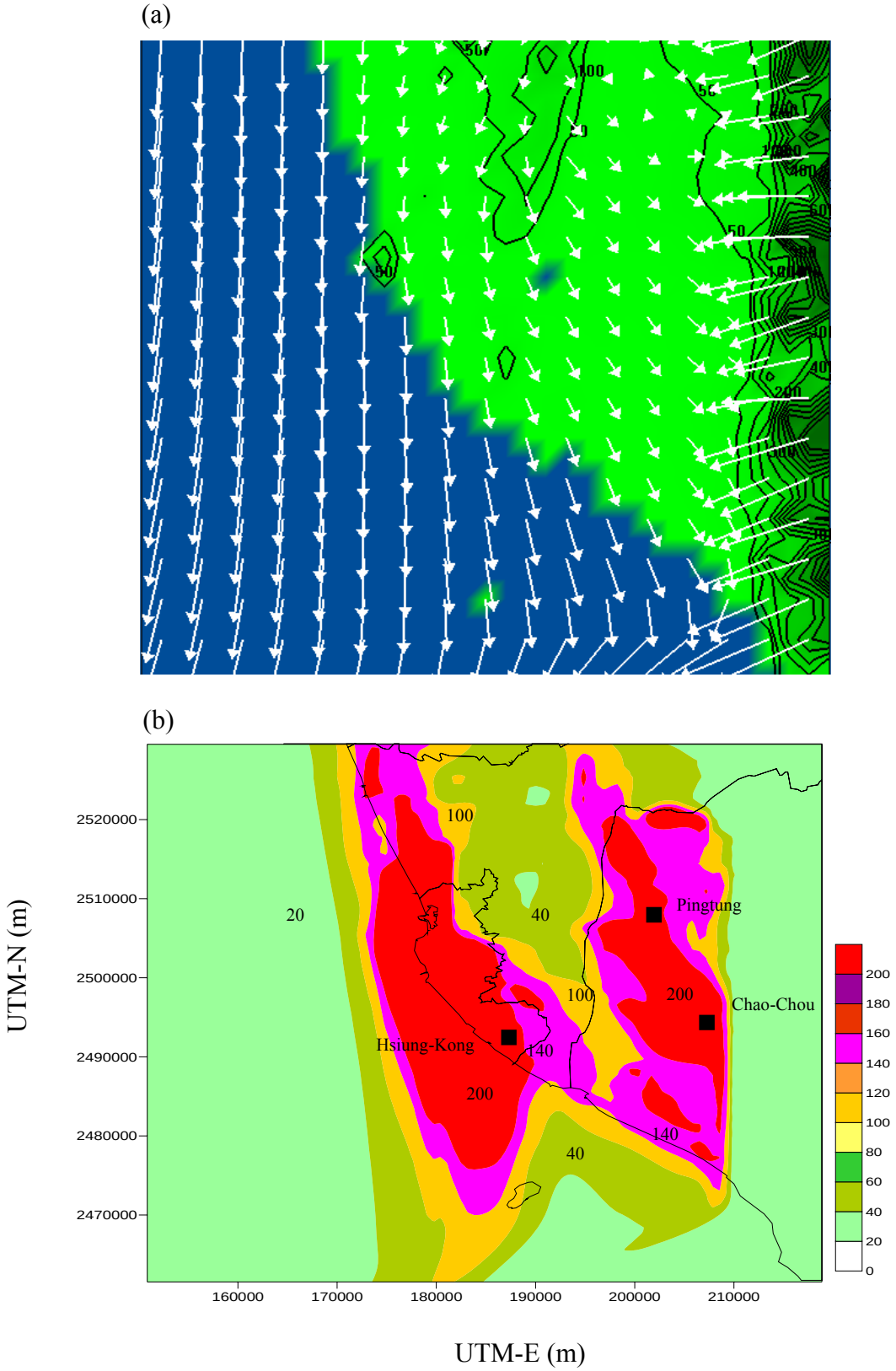

Fig. 9. (a) Simulated surface wind vectors, and (b) simulated concentration contours of PM_{10} at 20:00 on December 17, 2005.

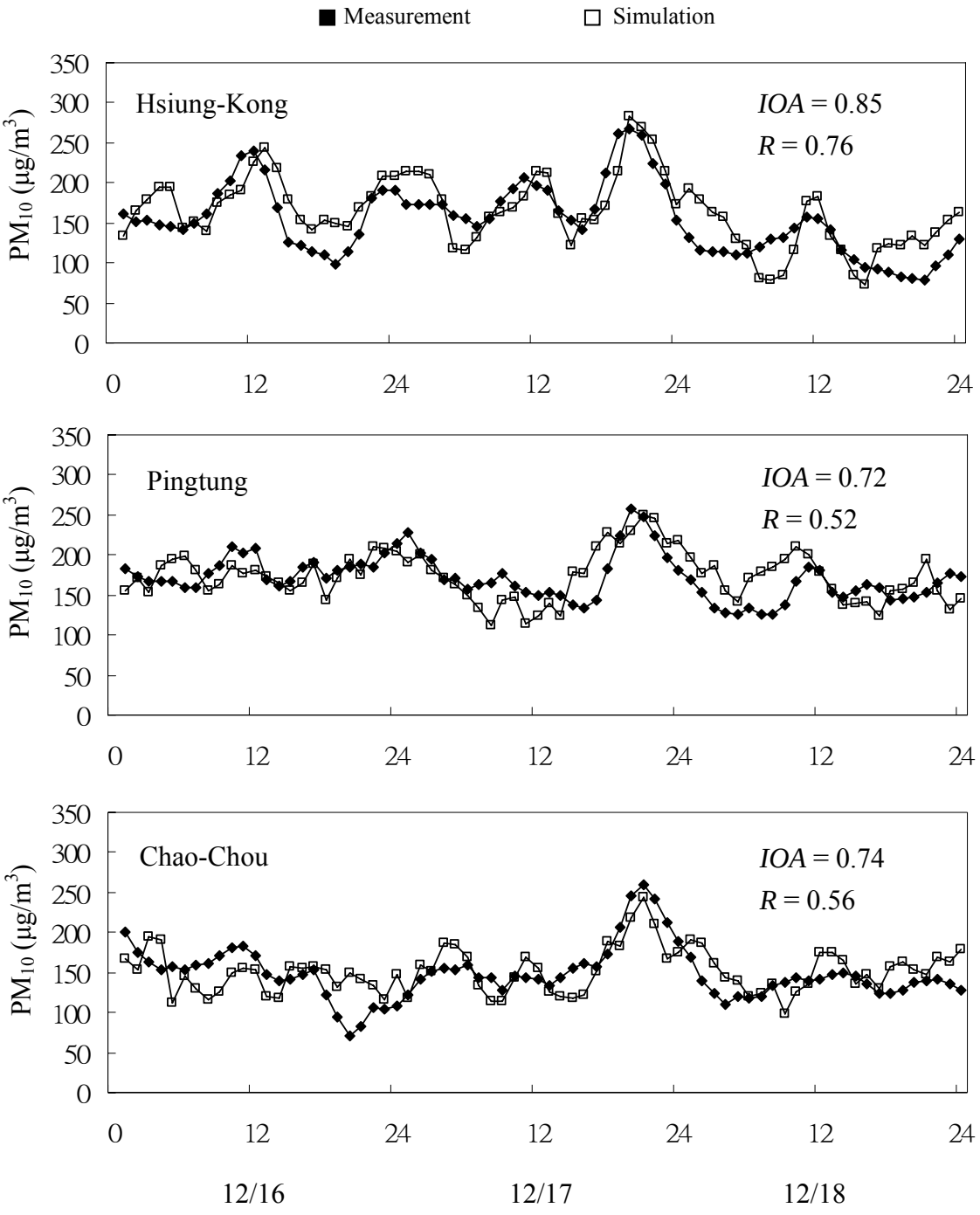

Fig. 10. Comparisons between hourly simulations of surface PM_{10} concentrations and measured concentrations at the Hsiung-Kong, Pingtung and Chao-Chou sites during December 16–18, 2005.

with measured concentrations at the three sites during December 16–18, 2005. The PM_{10} concentrations were relatively high at midnight. The highest (and mean) measured concentration was about 283 (164) μg/m^3 at the Hsiung-Kong site, 250 (174) μg/m^3 at the Pingtung site, and 243 (152) μg/m^3 at the Chao-Chou site. High PM_{10} pollution events

in winter were also associated with high-pressure systems and weak winds. In additional to even relatively higher pressures and weaker winds, the dry atmosphere in winter resulted in PM_{10} concentrations in the winter were higher than those in spring and winter. Simulated concentrations also agreed well with measured values, with R = 0.52–0.76 and IOA = 0.72–0.85.

Source contributions at three sites

The contribution of a particular source type to PM_{10} concentrations at one site can be estimated by re-running the TAPM model with emissions for that source at that region removed and comparing the simulated results with those obtained from the original emission inventory. Table 2 shows some similar and dissimilar features of source contributors among the three sites. Point (or industrial) sources contributed most (49.1%) to PM_{10} concentrations at Hsiung-Kong site (industrial), followed by area sources (35.0%), neighboring areas (7.8%), and traffic emissions (8.1%). Note that the neighboring areas of Hsiung-Kong site include Kaohsiung County, Pingtung County, Tainan City and Tainan County. The neighboring areas of Pingtung or Chao-Chou site include Kaohsiung City, Kaohsiung County, Tainan City and Tainan County. Conversely, neighboring areas (39.1% at Pingtung; 48.7% at Chao-Chou) and area sources (47.4% at Pingtung; 39.4% at Chao-Chou) contributed most to PM_{10} concentrations, followed by traffic emissions (5.8–9.0%) and point sources (4.5–6.1%) at the two sites. Since Pingtung and Chao-Chou are downwind of the Kaohsiung area when north or northeasterly winds prevail, PM_{10} from neighboring regions contributed about 44% at the two sites, significantly higher than that (about 8%) at the Hsiung-Kong (upwind) site.

CONCLUSIONS

Mesoscale simulations using the TAPM model were performed on the PM_{10} episodes in southern Taiwan in spring, autumn and winter of 2005. Predictions of hourly PM_{10} concentrations agree well with measured values at three monitoring sites (Hsiung-Kong, Pingtung and Chao-Chou). The synoptic weather chart indicated that prevailing winds were northwest (spring),

Table 2. Estimated source contributions at industrial, urban, and rural sites.

Monitoring Sites	Area Sources (%)			Line Sources (%)		Point Sources (%)	Neighboring Areas (%)
	Paved Road	Unpaved Road	Others	Gasoline Vehicles	Diesel Vehicles		
Hsiung-Kong	20.7	0.0	14.3	4.4	3.7	49.1	7.8
Pingtung	21.2	5.2	21.0	4.7	4.3	4.5	39.1
Chao-Chou	18.9	5.1	15.4	2.7	3.1	6.1	48.7

north (autumn), and northeasterly (winter). Meteorological conditions reveal that ambient PM_{10} typically accumulate and trigger episodes on days with high-surface pressure and weak winds.

Estimations using TAPM model indicate that industrial (point sources) emissions are the dominant contributors (about 49.1%) to PM_{10} concentrations at the Hsiung-Kong site in Kaohsiung City, followed by area sources (about 35.0%) and transport (about 7.8%) from neighboring counties, including Kaohsing County, Pintung County, and Tainan area. Because Pingtung City and Chao-Chou town are downwind of Kaohsiung City when north or northeasterly winds prevail, the two sites also experience high pollution events despite the fact that these two sites have few industrial pollutant sources; neighboring transport of PM_{10} to the two sites is extremely important, accounting for about 39.1% to PM_{10} concentrations at Pingtung and 48.7% at Chao-Chou. Since traffic emissions contributed little (around 7.8%) to PM_{10} concentrations at the three sites, reducing PM_{10} emissions from industrial sources in Kaohsiung City should be an effective way for improving air quality in Kaohsiung City, and in downwind areas, such as Pingtung County.

ACKNOWLEDGMENTS

The authors would like to thank the Environmental Protection Administration and the National Science Council in Taiwan for financially supporting this work under Contract No. NSC 94-EPA-Z-110-001 and NSC 95-EPA-Z-110-001.

REFERENCES

Arditsoglou, A. and Samara, C. (2005). Levels of Total Suspended Particulate Matter and Major Trace Elements in Kosovo: a Source Identification and Apportionment Study. *Chemosphere* 59: 669–678.

Chang, M.E. and Cardelino, C. (2000). Application of the Urban Airshed Model to Forecasting Next-day Peak Ozone Concentrations in Atlanta, Georgia. *J. Air and Waste Manage. Assoc.* 50: 2010–2024.

Chen, K.S., Ho, Y.T., Lai, C.H. and Chou Y.M. (2003). Photochemical Modeling and Analysis of Meteorological Parameters During Ozone Episodes in Kaohsiung, Taiwan. *Atmos. Environ.* 37 : 1811–1823.

Chen, K.S., Ho, Y.T., Lai, C.H., Tsai, Y.A. and Chen, S.J. (2004). Trends in Concentration of Ground-Level Ozone and Meteorological Conditions during High Ozone Episodes in Kao-Ping Airshed, Taiwan, *J. Air and Waste Manage. Assoc.* 54: 36–48.

Cheng, S., Chen, D., Li, J., Wang, H. and Guo, X. (2007). The Assessment of Emission-source Contributions to Air Quality by Using a Coupled MM5-ARPS-CMAQ Modeling System: A Case Study in the Beijing Metropolitan

Region, *China. Environ. Modelling and Software* 22: 1601–1616.

Cheng, M.D., Gao, N. and Hopke, P.K., (1996). Source Apportionment Study of Nitrogen Species Measured in Southern California in (1987). *J. Environ. Eng.* 122: 183–190.

Hurley, P.J., Blockley, A. and Rayner, K. (2001). Verification of a Prognostic Meteorological and Air Pollution Model for Year-long Predictions in the Kwinana Industrial Region of Western Australia. *Atmos. Environ.* 35: 1871–1880

Hurley, P. (2002). The Air Pollution Model (TAPM) Version 2. Part 1: Technical Description. CSIRO Atmospheric Research, Private Bag 1, Aspendale, Vic 3195, Australia.

Hurley, P., Manins, P., Lee, S., Boyle, R., Ng, Y.L. and Dewundege, P. (2003). Year-long, High-resolution, Urban Airshed Modelling: Verification of TAPM Predictions of Smog and Particles in Melbourne, Australia. *Atmos. Environ.* 37: 1899–1910.

Hurley, P.J., Physick, W.L. and Luhar, A.K., (2005). TAPM: A Practical Approach to Prognostic Meteorological and Air Pollution Modeling. *Environ. Modelling and Software* 20: 737–752.

Hurley, P. (2005). The Air Pollution Model (TAPM) Version 3. Part 1: Technical Description. CSIRO Atmospheric Research Technical NO. 71.

Johnson, G.M. (1984). A Simple Model for Predicting the Ozone Concentration of Ambient Air, *Proceedings of the 8th International Clean Air and Environment Conference*, New Zealand, Clean Air Society of Australia and New Zealand.

Luhar, A.K., Galbally, I.E. and Keywood, M., (2006). Modelling PM_{10} Concentrations and Carrying Capacity Associated with Woodheater Emissions in Launceston, Tasmania. *Atmos. Environ.* 40: 5543–5557.

Lin, J.J. and Lee, L.C., (2004). Characterization of the Concentration and Distribution of Urban Submicron (PM_{10}) Aerosol Particles. *Atmos. Environ.* 38: 469–475.

Park, I.S., Lee, S.J., Kim, C.H., Yoo, C. and Lee, Y.H. (2004) Simulating Urban-scale Air Pollutants and their Predicting Capabilities Over the Seoul Metropolitan Area. *J. Air and Waste Manage. Assoc.* 54: 695–710.

So, K.L. and Wang, T., (2004). C3–C12 Non-methane Hydrocarbons in Subtropical Hong Kong: Spatial-temporal Variations, Source-receptor Relationships and Photochemical Reactivity. *Sci. of Total Environ.* 328: 161–174.

Stauffer, D.R. and N. Seaman, (1994). Multiscale four Dimensional Data Assimilation. *J. App. Meteor.* 33: 416–434.

Viana. M., Querol, X., Alastuey, A., Gil, J.I. and Menendez, M. (2006). Identification of PM Sources by Principal Component Analysis (PCA) Coupled with Wind Direction Data. *Chemosphere* 65: 2411–2418.

Wang, H. and Shooter, D. (2004). Low

Molecular Weight Dicarboxylic Acids in PM_{10} in a City with Intensive Solid Fuel Burning. *Chemosphere* 56: 725–733.

Willmott, C.J., Ackleson, S.G., Davis, R.E., Feddema, J.J., Klink, K.M., Legates, D.R., O'Donnell, J. and Rowe, C.M. (1985). Statistics for the Evaluation and Comparisons of Model. *J. Geophys. Res.* 90: 8995–9005.

Wilson, J.G. and Zawar-Reza, P. (2006). Intraurban-scale Dispersion Modelling of Particulate Matter Concentrations: Applications for Exposure Estimates in Cohort Studies. *Atmos. Environ.* 40: 1053–1063

Zawar-Reza, P., Kingham, S. and Pearce, J. (2005). Evaluation of a Year-long Dispersion Modelling of PM_{10} Using the Mesoscale Model TAPM for Christchurch, New Zealand. *Sci. Total Environ.* 349: 249–259.

Received for review, June 16, 2008
Accepted, July 24, 2008